

Supporting Information

**A Porous, Electrically Conductive Hexa-
Zirconium(IV) Metal-Organic Framework**

*Subhadip Goswami,[†] Debmalaya Ray,[‡] Ken-ichi Otake,[†] Chung-Wei Kung,[†] Sergio J. Garibay,[†]
Timur Islamoglu,[†] Ahmet Atilgan,[†] Yuexing Cui,[†] Christopher J. Cramer,[‡] Omar K. Farha,^{†, §},
Joseph T. Hupp^{†*}*

[†] Department of Chemistry, Northwestern University, 2145 Sheridan Road, Evanston, IL 60208, United States

[‡] Department of Chemistry, Chemical Theory Center, and Minnesota Supercomputing Institute, University of Minnesota, 207 Pleasant Street SE, Minneapolis, MN 55455

[§] Department of Chemistry, King Abdulaziz University, Jeddah 21589, Saudi Arabia

Section S1. Experimental Section

Materials

Fullerene (C₆₀), N,N-dimethylformamide (DMF), 4-aminobenzoic acid, hydrochloric acid (HCl, 37%), acetone were purchased from sigma aldrich and used without any further purification. The linker TBAPy was synthesized according to the literature procedure and the chemicals used were the same as reported before.¹

Instrumentation

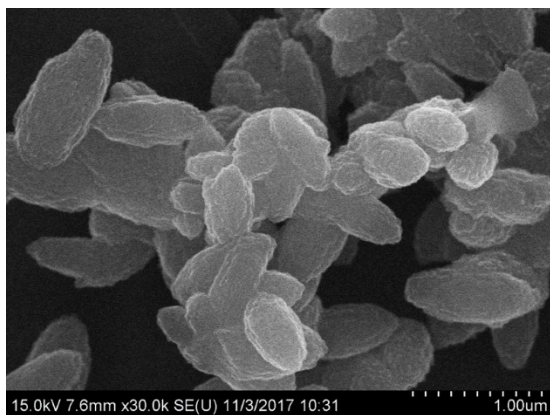
Powder X-ray diffraction (PXRD) data were collected on a STOE-STADIMP powder diffractometer equipped with an asymmetric curved Germanium monochromator (CuK α 1 radiation, $\lambda = 1.54056 \text{ \AA}$) and one dimensional silicon strip detector (MYTHEN2 1K from DECTRIS). The line focused Cu X-ray tube was operated at 40 kV and 40 mA. The activated MOF samples of **NU-901** and **NU-901-C₆₀** were packed into a metallic mask with a 3 mm diameter hole and the samples were encapsulated between layers of Kapton tape. The holder was spun and diffraction intensity data were collected in a transmission geometry mode. Intensity data from 1 to 20 degrees 2 θ were collected over a period of 30 mins. The instrument was calibrated against a NIST Silicon standard (640d). Nitrogen isotherm measurements were performed on a Micromeritics Tristar II 3020 (Micromeritics, Norcross, GA) instrument at 77 K with 30 mg- 50 mg of MOF samples. Before isotherm measurement, the MOF samples were activated at 120 °C under vacuum for 12 h on Micromeritics Smart VacPrep instrument. Scanning electron microscopy (SEM) images were collected on a Hitachi SU8030 instrument. The samples were prepared by coating ~9 nm of OsO₄ on MOF samples in in a Denton Desk III TSC Sputter Coater (Moorestown, NJ). Raman spectra of the samples were measured on a Horiba LabRAM HR Confocal Raman system. A small amount of sample was placed on a glass

slide and was excited at 785 nm through a 50% ND filter for 120 s. Each sample was scanned over two times to obtain the spectrum. The UV-Vis spectra for estimation of C₆₀ loading was measured on a Cary 5000 UV-VIS-NIR spectrophotometer. Diffuse reflectance UV-Vis spectra (DRUV-vis; Shimadzu UV-3600) of the MOF samples were carried out from 700 to 200 nm with a Harrick Praying Mantis diffuse reflectance accessory. The baseline measurement was performed with polytetrafluoroethylene (PTFE) powder as a perfect reflector. The steady state fluorescence of the MOF samples were measured with Photon Technology International (PTI) QuantaMaster 400 fluorometer. The electrical conductivity measurements on pressed-pellets were conducted on a Solarton Analytical Modulab Potentiostat and CHI 660 electrochemical workstation (CH Instruments, Inc., USA). The I-V curves on interdigitated electrodes (IDEs) were measured on a CHI 900 potentiostat (CH Instruments, Inc., USA) with a two electrode set up connected to a drop-cell connector (MicruX Technologies, ED-DROP-CELL). All of the I-V curves were measured in air at room temperature.

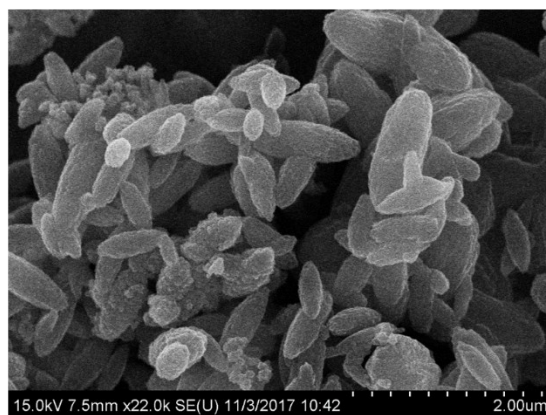
Section S2. Synthesis of NU-901-C₆₀

NU-901-C₆₀: 32 mg (10 equivalent) of Fullerene (C₆₀) was dissolved in 2 mL of o-dichlorobenzene and activated NU-901 (10 mg) was added to it. The vial was then placed in a preheated oven at 60°C for 4 days. After that the vial was cooled down to room temperature and the supernatant was decanted. The obtained MOF sample was washed with o-dichlorobenzene (3 x 7 mL-in between soaking time 2 h) extensively to remove any physisorbed C₆₀ on the MOF surface and with acetone (3 x 7 mL-in between soaking time 2 h). The solid was then dried under dynamic vacuum at 120°C for 12 h.

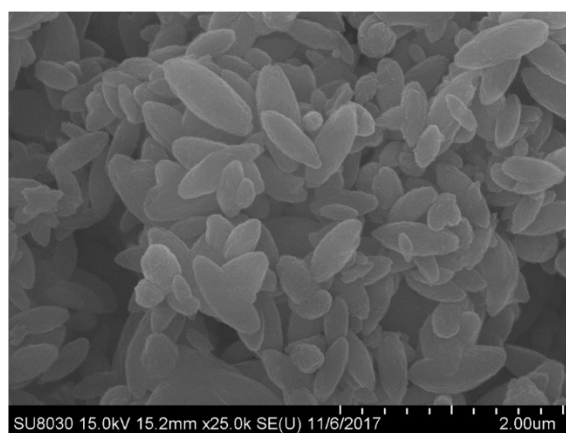
NU-901-Amino-C₆₀: The synthesis procedure for NU-901-Amino-C₆₀ is similar to NU-901-C₆₀ where NU-901-Amino was used to encapsulate C₆₀.



NU-901-C₆₀



NU-901



NU-901-Amino-C₆₀

Figure S1. Scanning electron microscopy images of NU-901-C₆₀, NU-901 and NU-901-Amino-C₆₀.

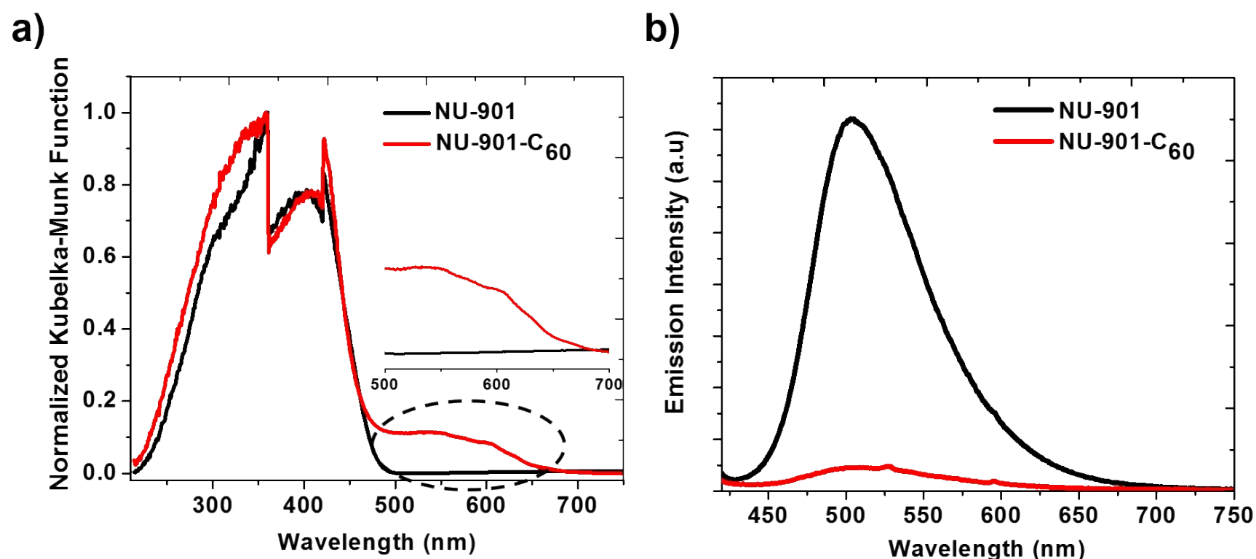


Figure S2. a) Diffuse reflectance UV-vis spectra of NU-901 and NU-901-C₆₀, b) steady state emission spectra of NU-901 and NU-901-C₆₀. The samples were excited at 390 nm to collect the spectra.

Section S3. Preparation of MOF coated interdigitated electrodes (IDEs) for I-V curve measurement

The interdigitated electrodes (IDEs) with 180 pairs of platinum fingers and a 5- μ m gap (MicruX Technologies, ED-IDE3-Pt) were used to obtain the current (I)-voltage (V) plots. First, the MOFs were taken in acetone and sonicated to make a uniform dispersion at a concentration of 10 mg/mL. Thereafter, 2 μ L of the suspension was drop casted on IDE to make a uniform coverage of thin film. The MOF-coated electrodes were then air dried overnight before taking the I-V measurement.

Section S4. Fabrication of MOF-pellets for electrical conductivity measurement

The DMF soaked MOFs were filtered with filter paper and the amount of vacuum applied was just enough to dry the sample to transfer in a vial. The powder was then transferred to a Thermo Fisher Scientific 7 mm die set and 500 psi pressure was applied to obtain a pellet with a

thickness of 400 μM . Solvent exchange with acetone was performed by soaking the pellet in acetone for 24 h and exchanging the solvent five times with 1 h interval time. To measure the N_2 adsorption-desorption isotherm, the pellet was activated under vacuum at 120°C for 12 h and the isotherm was measured at 77 K.

Conductive epoxy was applied to both sides of the pressed MOF pellet and sandwiched between two conductive cleaned FTO substrates. The conductivity of the pellet was then measured by two-point probe technique using equation S1-

$$\sigma = \frac{I}{V} \cdot \frac{L}{A} \quad (\text{Equation S1})$$

Where the ratio of I/V is obtained from the slope of I-V plot and the area is calculated considering the diameter of 7 mm. The value of L is 400 μm .

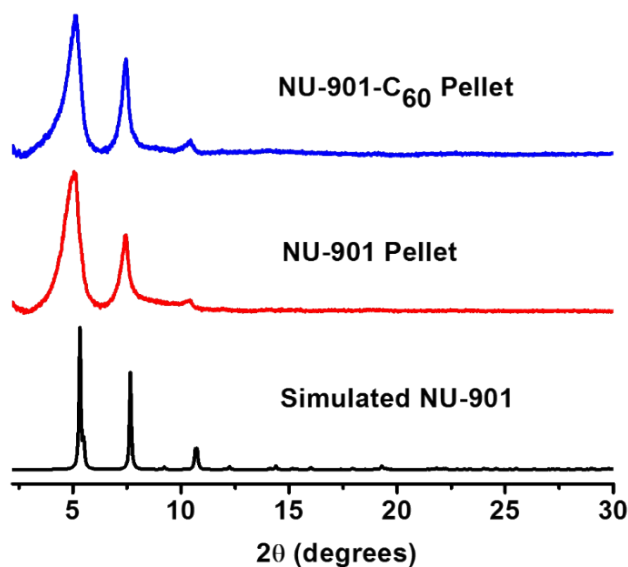


Figure S3. PXRD patterns of simulated NU-901 along with NU-901 pellet and NU-901- C_{60} pellet.

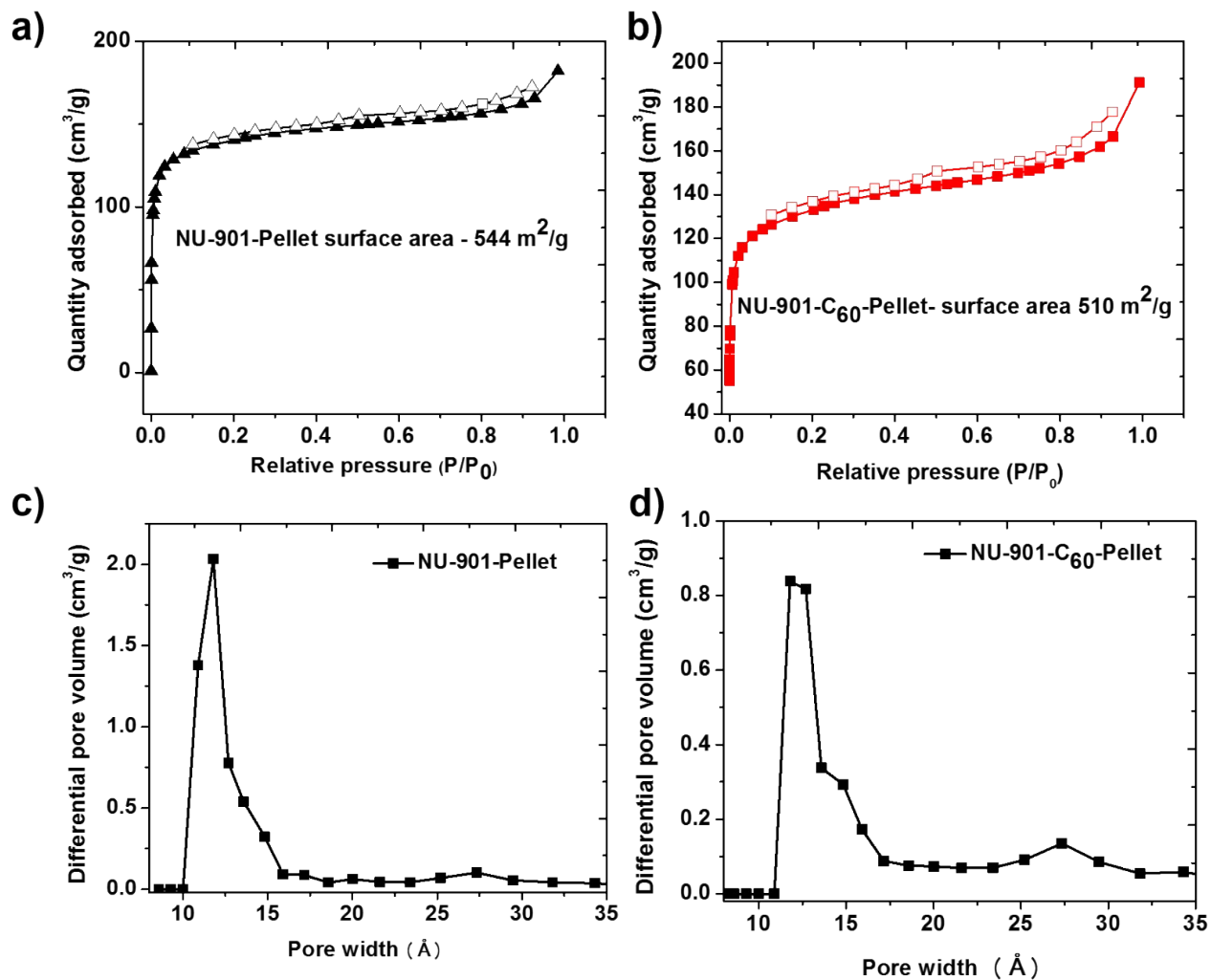


Figure S4. Nitrogen adsorption and desorption isotherms (a and b) and DFT pore-size-distribution plots (c and d) for NU-901 and NU-901-C₆₀ pellets.

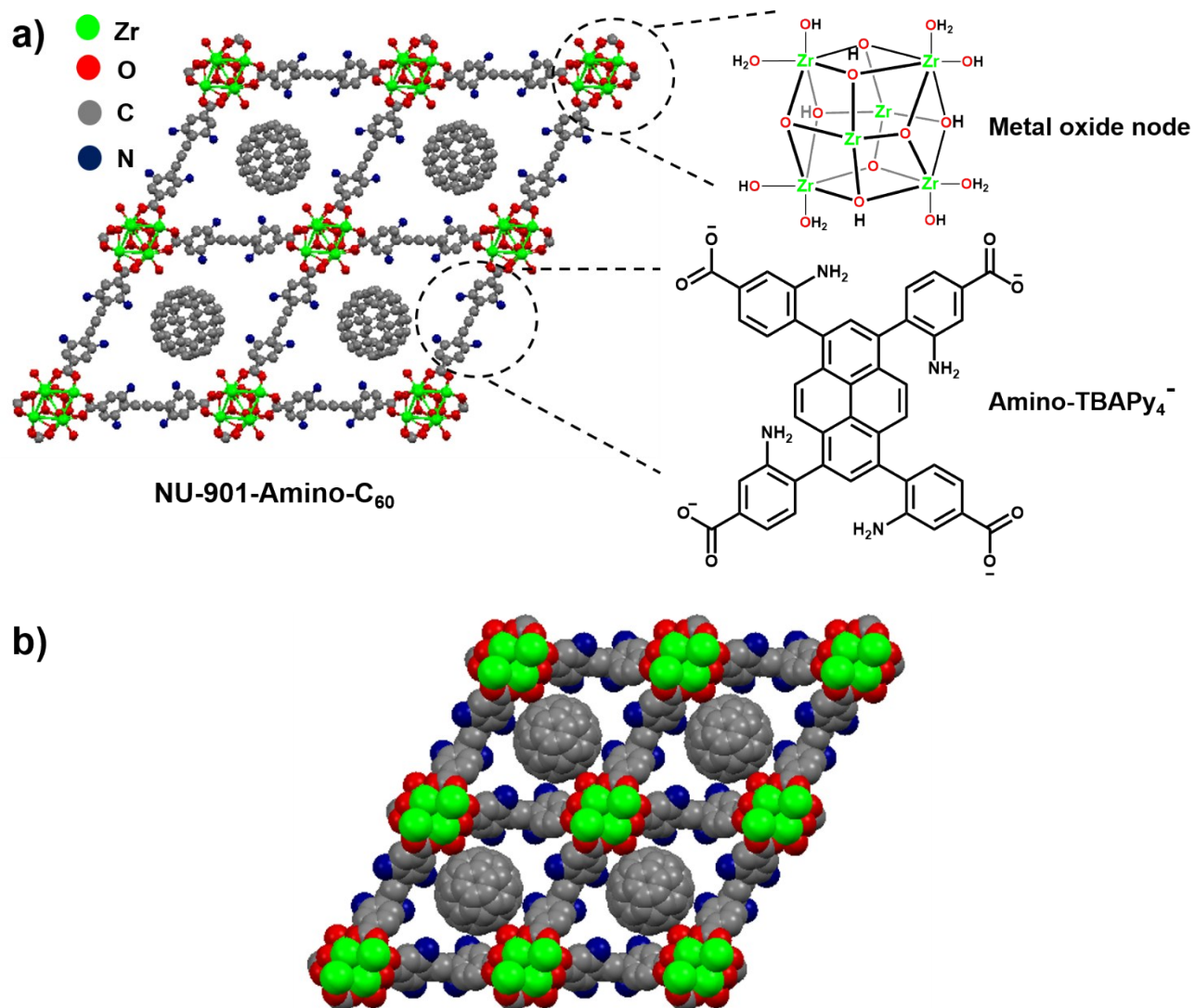


Figure S5. a) Simulated structure of NU-901-Amino-C₆₀ showing the structure of the metal node and the linker, b) space-filled model of NU-901-Amino-C₆₀.

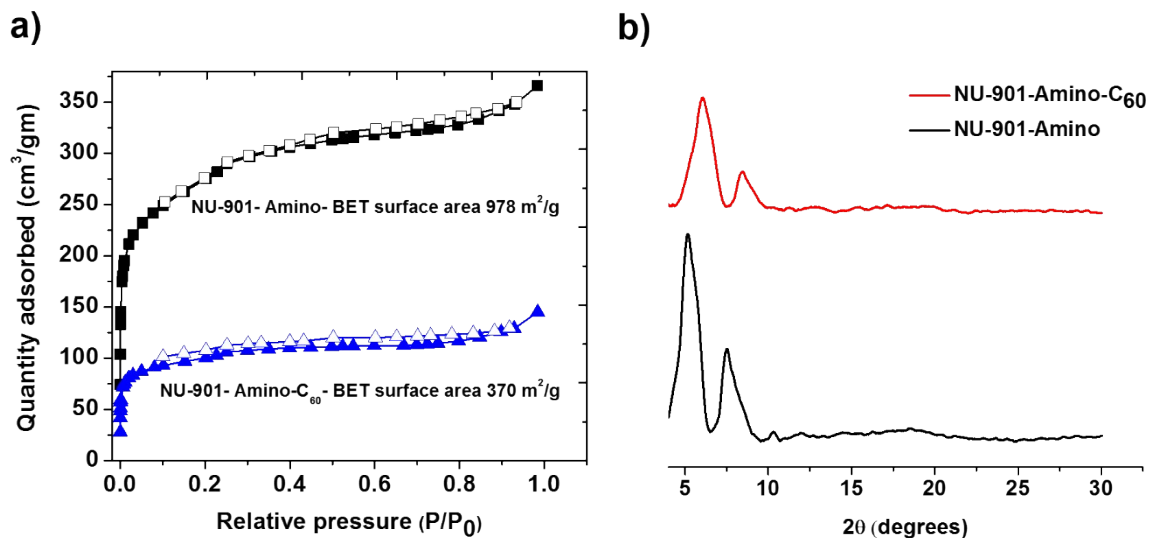


Figure S6. a) Nitrogen adsorption-desorption isotherms and b) PXRD patterns of NU-901-Amino and NU-901-Amino-C₆₀.

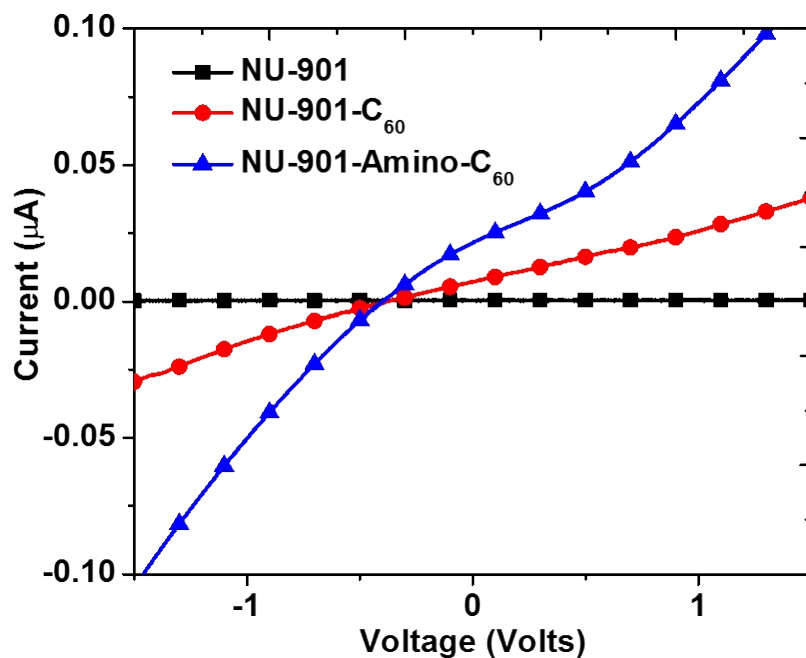


Figure S7. Current (I) vs Voltage (V) plots for NU-901, NU-901-C₆₀ and NU-901-Amino-C₆₀. Scans were initiated at -2 V with a rate of 50 mV/s. The offset of the zero-current point from zero bias is tentatively ascribed to hysteresis in the I-V curves with a similar voltage offset of opposite sign, anticipated for scans in the reverse direction. Unfortunately, we lack sufficient samples to explore this point here, but will return to it in follow up studies.

Section S5. Computational details

Structures of NU-901 and NU-901-modified-linker with and without C_{60} was optimized using VASP package.²⁻⁵ Projector augmented wave pseudopotential (PAW)^{6, 7} was used for our calculations. All the periodic calculations were performed using PBE^{8, 9} functional along with Becky-Johnson dispersion correction.^{10, 11} We used a plane wave energy cut off of 520 eV for structural optimization and a gamma centered k-point grid of 2*2*2 was used for sampling the Brillouin zone. Energy convergence criteria of 10^{-5} eV and force convergence criteria of 0.02 eV/Å was used for our calculations. Density of states calculations were performed in VASP using the optimized periodic structures.

For the charge transfer calculation, we cut clusters of NU-901 and C_{60} complex from the periodic structure and truncated the carboxylate groups with hydrogen atoms and optimized only the position of additionally added hydrogens were optimized using ADF software package¹² using PBE-D3 functional and TZP all electron basis set. The M06-2X functional¹³ with TZP all electron basis set was used for calculating charge transfer integrals. We used fragment based approach as implemented in ADF package for charge transfer calculations.^{14, 15}

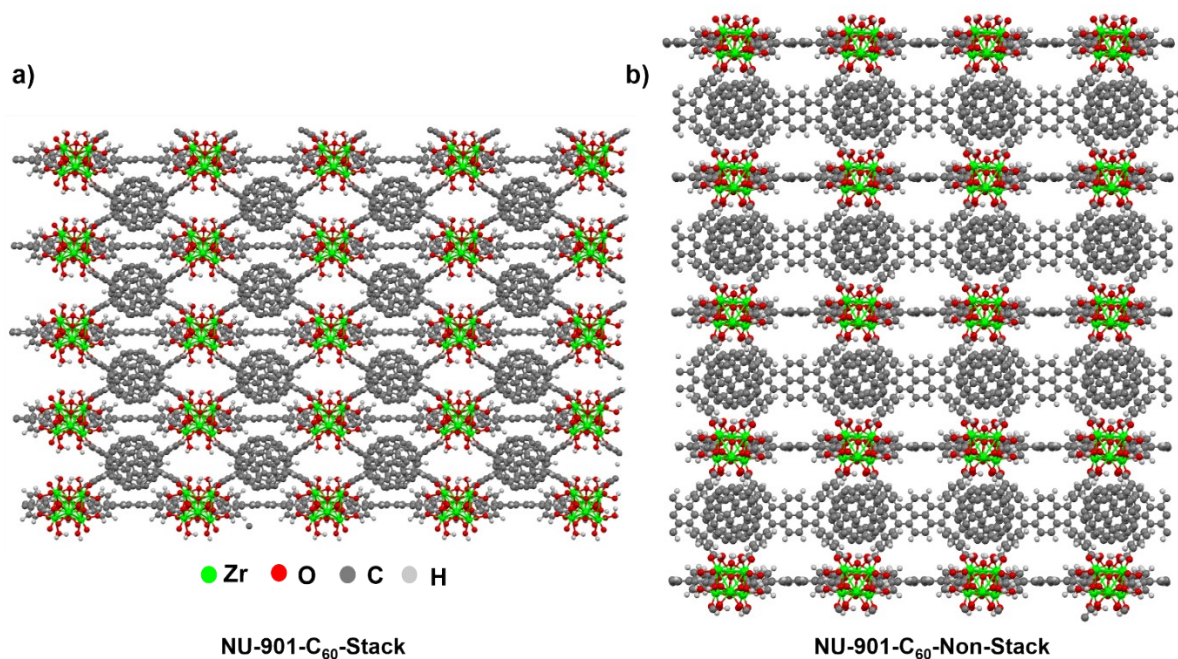
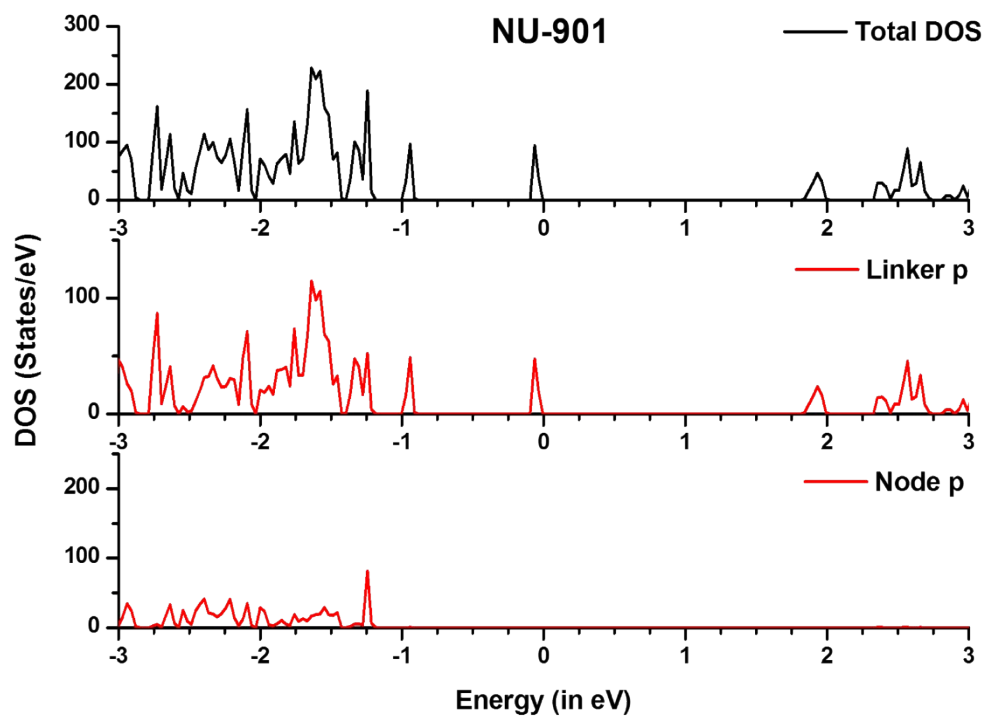
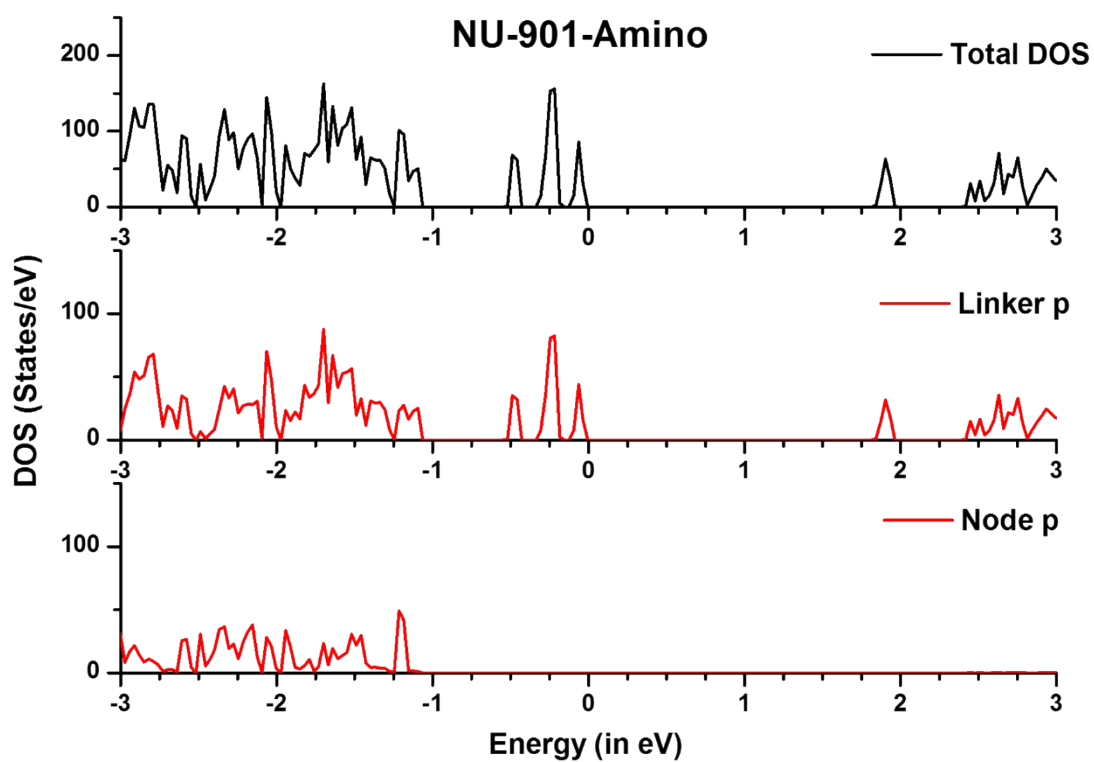
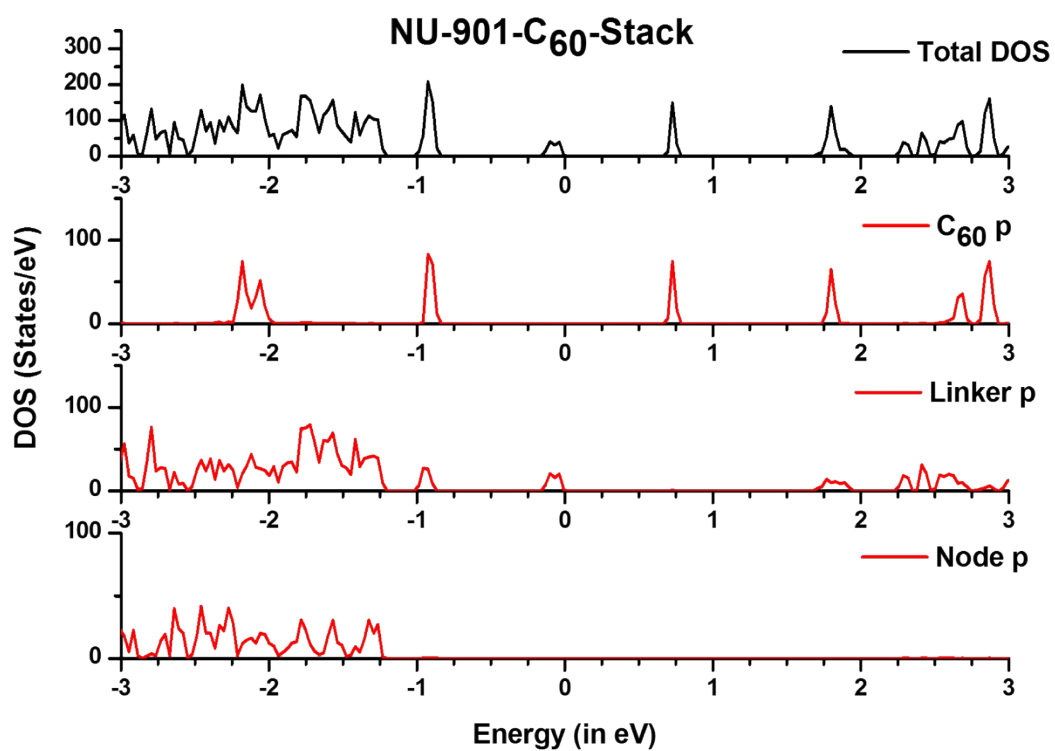


Figure S8. a) Simulated structure of NU-901-C₆₀-Stack (C₆₀ stacked with TBAPy₄⁻), **b)** NU-901-C₆₀-Non-Stack (C₆₀ not stacked with TBAPy₄⁻) along crystallographic *b* axis.





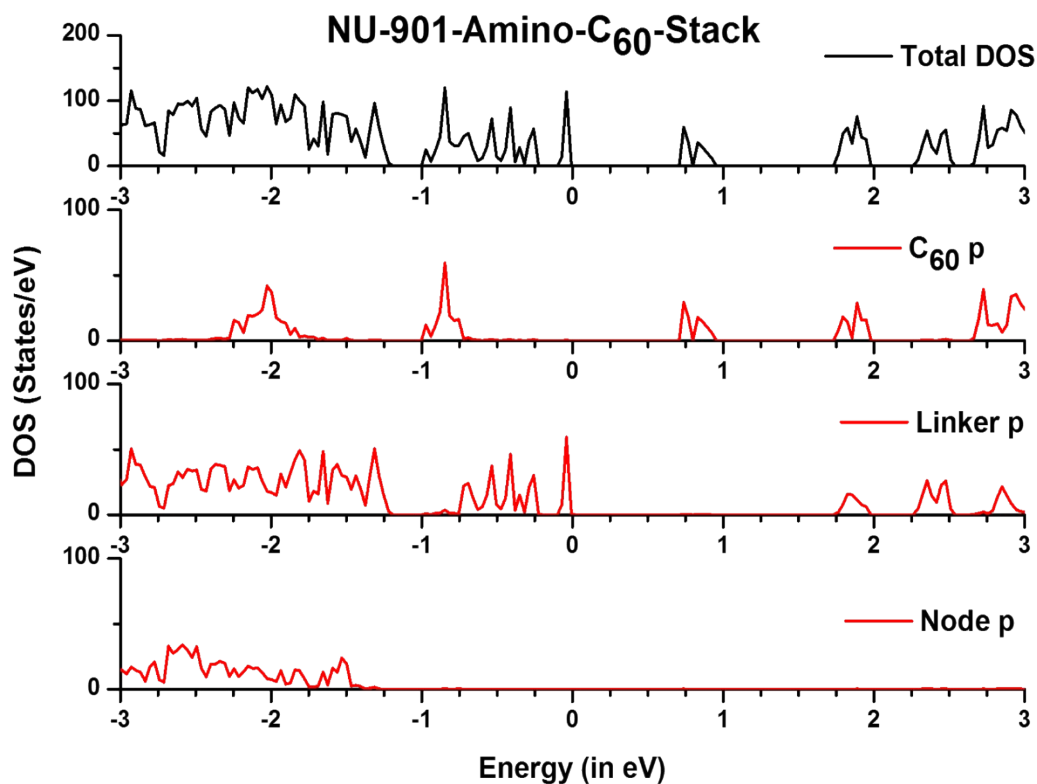


Figure S9. Calculated and projected density of states (DOS) for pristine NU-901, NU-901-Amino and for C₆₀ infiltrated MOFs of NU-901-C₆₀, NU-901-Amino-C₆₀ in stacked conformation.

Table S1. Hole transfer and electron transfer integrals of NU-901-C₆₀-Stack and NU-901-Amino-C₆₀-Stack

MOF structure	Hole Transfer Integral (cm ⁻¹)	Electron Transfer Integral (cm ⁻¹)
NU-901-C ₆₀ -Stack	18.8	29.6
NU-901-Amino-C ₆₀ -Stack	71.6	61.5

References

1. J. E. Mondloch, W. Bury, D. Fairen-Jimenez, S. Kwon, E. J. DeMarco, M. H. Weston, A. A. Sarjeant, S. T. Nguyen, P. C. Stair, R. Q. Snurr, O. K. Farha and J. T. Hupp, *J. Am. Chem. Soc.*, 2013, **135**, 10294.
2. G. Kresse and J. Furthmüller, *Computational Materials Science*, 1996, **6**, 15.
3. G. Kresse and J. Furthmüller, *Phys. Rev. B*, 1996, **54**, 11169.
4. G. Kresse and J. Hafner, *Phys. Rev. B*, 1993, **47**, 558.
5. G. Kresse and J. Hafner, *Phys. Rev. B*, 1994, **49**, 14251.
6. P. E. Blöchl, *Physical Review B*, 1994, **50**, 17953.
7. G. Kresse and D. Joubert, *Phys. Rev. B*, 1999, **59**, 1758.
8. J. P. Perdew, K. Burke and M. Ernzerhof, *Phys. Rev. Lett.*, 1996, **77**, 3865.
9. J. P. Perdew and Y. Wang, *Phys. Rev. B*, 1992, **45**, 13244.
10. A. D. Becke and E. R. Johnson, *J. Chem. Phys.*, 2005, **123**, 154101.
11. S. Grimme, J. Antony, S. Ehrlich and H. Krieg, *J. Chem. Phys.*, 2010, **132**, 154104.
12. G. te Velde, F. M. Bickelhaupt, E. J. Baerends, C. Fonseca Guerra, S. J. A. van Gisbergen, J. G. Snijders and T. Ziegler, *J. Comput. Chem.*, 2001, **22**, 931.
13. Y. Zhao and D. G. Truhlar, *Theor. Chem. Acc.*, 2008, **120**, 215.
14. K. Senthilkumar, F. C. Grozema, F. M. Bickelhaupt and L. D. A. Siebbeles, *J. Chem. Phys.*, 2003, **119**, 9809.
15. K. Senthilkumar, F. C. Grozema, C. F. Guerra, F. M. Bickelhaupt, F. D. Lewis, Y. A. Berlin, M. A. Ratner and L. D. A. Siebbeles, *J. Am. Chem. Soc.*, 2005, **127**, 14894.